Biomaterials 37 (2015) 367–382

Contents lists available at ScienceDirect

Biomaterials

journal homepage: www.elsevier.com/locate/biomaterials

Fluorescent cell-traceable dexamethasone-loaded liposomes for the treatment of inflammatory liver diseases

Matthias Bartneck [a, 1], Katharina M. Scheyda [a, 1], Klaudia T. Warzecha [a], Larissa Y. Rizzo [b], Kanishka Hittatiya [c], Tom Luedde [a], Gert Storm [d, e], Christian Trautwein [a], Twan Lammers [b, d, e], Frank Tacke [a, *]

[a] Department of Medicine III, Medical Faculty, RWTH Aachen, Pauwelsstr. 30, 52074 Aachen, Germany
[b] Department of Experimental Molecular Imaging (ExMI), Helmholtz Institute for Biomedical Engineering, Medical Faculty, RWTH Aachen, Pauwelsstr. 30, 52074 Aachen, Germany
[c] Institute of Pathology, University Bonn, Sigmund-Freud-Str. 25, 53127 Bonn, Germany
[d] Department of Controlled Drug Delivery, MIRA Institute for Biomedical Technology and Technical Medicine, University of Twente, PO Box 217, 7500 AE Enschede, The Netherlands
[e] Department of Pharmaceutics, Utrecht Institute for Pharmaceutical Sciences (UPIS), Universiteitsweg 99, 3584 CG Utrecht, The Netherlands

ARTICLE INFO

Article history:
Received 1 August 2014
Accepted 2 October 2014
Available online 26 October 2014

Keywords:
Macrophages
T cells
Liposomes
Dexamethasone
Liver injury
Liver fibrosis

ABSTRACT

Liposomes are routinely used carrier materials for delivering drug molecules to pathological sites. Besides in tumors and inflammatory sites, liposomes also strongly accumulate in liver and spleen. The potential of using liposomes to treat acute and chronic liver disorders, however, has not yet been evaluated. We here explored the therapeutic potential of dexamethasone (Dex)-loaded liposomes for inflammatory liver diseases, using experimental models of acute and chronic liver injury in mice. Fluorescently labeled liposomes predominantly accumulated in hepatic phagocytes, but also in T cells. Importantly, Dex-loaded liposomes reduced T cells in blood and liver, more effectively than free Dex, and endorsed the anti-inflammatory polarization of hepatic macrophages. In experimental chronic liver damage, Dex-loaded liposomes significantly reduced liver injury and liver fibrosis. In immune-mediated acute hepatitis Dex-loaded liposomes, but not free Dex, significantly reduced disease severity. T cells, not macrophages, were significantly depleted by Dex liposomes in liver disease models *in vivo*, as further supported by mechanistic cell death *in vitro* studies. Our data indicate that Dex liposomes may be an interesting treatment option for liver diseases, in particular for immune-mediated hepatitis. The depletion of T cells might represent the major mechanism of action of Dex liposomes, rather than their macrophage-polarizing activities.

1. Introduction

Liposomes are nano-sized biodegradable drug delivery systems that can be used for a targeted, cell-specific administration of drugs with reduced systemic side effects. The increased efficacy and reduced toxicity of drugs upon liposomal encapsulation has been convincingly established for anti-cancer chemotherapeutics, for instance, for the cytostatic drug doxorubicin [1]. Liposomal drug delivery is also considered to be potentially beneficial for the treatment of inflammatory diseases [2], because the systemic administration of anti-inflammatory drugs regularly results in systemic immunosuppression rendering patients susceptible for infections such as sepsis [3]. We have previously shown that liposomal encapsulation of the anti-inflammatory drug dexamethasone allows for a reduction of unspecific effects of the encapsulated compounds on human primary cells [4].

Corticosteroids are routinely used to treat inflammatory liver diseases, such as autoimmune hepatitis and alcoholic hepatitis [5,6]. At present, no liposomal corticosteroid formulations have been approved for the treatment of liver diseases yet. As large quantities of nanoparticles translocate to the liver upon systemic application [7], nanoparticle-based drug delivery could represent a promising strategy for combatting liver diseases [8]. The accumulation of nanoparticles in the liver can be partially related to their internalization by hepatic macrophages, such as Kupffer cells,

* Corresponding author. Tel.: +49 2418035848.
E-mail address: frank.tacke@gmx.net (F. Tacke).
[1] These authors contributed equally.

http://dx.doi.org/10.1016/j.biomaterials.2014.10.030
0142-9612/

which are located at the fenestrated endothelium and which are in direct contact with blood [9]. Subsequent to their internalization by macrophages [10], nanoparticles are known to influence the state of hepatic macrophage polarization [11].

Macrophages exhibit a high plasticity with respect to their functions in regulating inflammation [12]. They can be polarized into either a proinflammatory M1 or an anti-inflammatory M2 macrophage subtype. Key molecular markers of M1 macrophages are tumor necrosis factor α (TNFα) and interleukin 1β (IL1β), whereas characteristic M2 markers are Arginase 1 (Arg1), resistin like alpha (Retnla, FIZZ-1) and IL4 [13]. M1 macrophages in diseased livers mainly originate from monocytes that translocate into the liver upon injury, and they express F4/80, CD11b and the Ly6C antigen on their surface, whereas Kupffer cells are resident liver macrophages, expressing high levels of F4/80 but low levels of Ly6C and CD11b [14]. Alternatively activated M2 macrophages exhibit characteristic surface markers such as the IL4 receptor α (CD124), which inhibits inflammation [15], the mannose receptor (CD206) and the macrophage C-type lectin domain family 10, member A (CLEC10A, CD301), all of which can potentially be regulated by targeted nanotherapeutics [11].

While many reports have underlined the importance of macrophages for interactions with nanoparticles *in vitro*, it has not been studied in great detail to which extent these observations translate into disease models *in vivo*. We have recently demonstrated that liposomes loaded with the corticosteroid dexamethasone block migratory and inflammatory functions of primary human macrophages *in vitro* [4]. We now investigated the effects of liposomal encapsulated dexamethasone on macrophages and other immune cell populations *in vivo*. Using fluorescently labeled and/or dexamethasone (Dex)-loaded liposomes for intravenous administration in mice, we characterized the biodistribution, toxicity, impact on immune cell numbers, and functions in the circulation and in the liver. We further evaluated the potential of Dex-loaded liposomes as therapeutics for treating hepatitis and liver fibrosis, employing experimental models of acute Concanavalin A (ConA)-based hepatitis and chronic toxic carbon tetrachloride (CCl_4)-based liver injury, respectively. As these data unexpectedly indicated that Dex liposomes primarily exert their anti-inflammatory actions via depleting T cells *in vivo*, we furthermore isolated primary murine lymphocytes as well as macrophages and explored cell-specific mechanisms of Dex liposome induced cell death.

2. Materials and methods

2.1. Liposome preparation and characterization

Liposomes were prepared based on the film-method [16]. Briefly, Dipalmitoyl phosphatidylcholine (DPPC) and PEG-(2000)-distearoyl phosphatidylethanolamine (PEG-(2000)-DSPE), obtained from Lipoid (Ludwigshafen, Germany), cholesterol, obtained from Sigma (St. Louis, MO, USA), and (N-(7-Nitrobenz-2-oxa-1,3-diazol-4-yl)-1,2-dihexadecanoyl-snglycero-3-phosphoethanolamine, triethyl-ammonium salt) (NBD-PE) was obtained from Molecular Probes (Grand Island, New York, USA). All other chemicals were of reagent grade. A mix of chloroform and methanol (volumetric ratio of 10:1) containing DPPC, PEG-(2000)-DSPE, NBD-PE, and cholesterol was prepared at a molar ratio of 1.85:0.15:0:1. One mol% of NBD-PE was added to the organic phase in relation to the total amount of lipid, including cholesterol. The organic phase was evaporated with a rotavapor (BUCHI Labortechnik AG, Flawil, Switzerland), followed by nitrogen flushing for removal of residual organic solvent. Hydration of the lipid film was done at 50 °C in an aqueous solution of dexamethasone phosphate in a concentration of 100 mg/mL and a phospholipid concentration of 100 mM. Liposomes without dexamethasone phosphate were dispersed in phosphate buffered saline (PBS). The liposomes were sequentially extruded through two stacked polycarbonate filters with pore sizes of 600, 200, and 100 nm (Nuclepore, Pleaston, USA) under nitrogen pressure, using a Lipex high pressure extruder (Lipex, Nortern Lipids, Vancouver, Canada), retrieving liposomes sizing 100 nm. Unencapsulated dexamethasone phosphate was cleared by dialysis at 4 °C against PBS using Slide-A-Lyzer dialysis cassettes (Pierce, Rockford, USA) with a molecular cut-off of 10 kD [11].

The mean particle size was determined by dynamic light scattering with an ALVCGS-3 system (Malvern Instruments, Worcestershire, United Kingdom). Thezeta potential was determined using a Zetasizer Nano Z (Malvern Instruments Ltd., Worcs, UK) and that of the PEGylated liposomes was 5.1 ± 1.4 mV. The phospholipid content was determined with a phosphate assay [17,18] on the organic phase after extraction of the liposomal preparation with chloroform. The aqueous phase after extraction was used to determine the liposomal dexamethasone phosphate concentration of the liposomes by high performance liquid chromatography using a mobile phase of acetonitrile/water of pH 2 at a ratio of 25/75 and monitoring the eluents with a UV-detector at 254 nm. A limulus amebocyte lysate (LAL) assay QCL-1000 obtained from Lonza (Walkersville, MD, USA) was used to test for possible endotoxin contaminations of the liposomes. The kit was used according to the instructions of the manufacturer.

2.2. Mice

C57BL6/J wild-type mice were housed in a specific pathogen-free environment. All experiments were done with male animals at 8–12 weeks of age under ethical conditions approved by the appropriate authorities according to German legal requirements. In an earlier *in vitro* study, we have used Dex at a concentration of 10 μg/mL with human primary immune cells. This concentration resembled a Dex concentration of 1 mg/kg body weight, based on the assumption that one mouse has a total body fluid volume (where liposomes can accumulate) of 2.5 mL, a comparative study that we have done earlier with gold nanorods [11,19]. For the cell culture experiments, the liposomes without Dex were diluted with sterile 0.9% sodium chloride solution to a phospholipid (PL) concentration of 77 nmol/mL, corresponding to a concentration of 77 μM PL in the cell culture medium. Thus, one mouse weighing 25 g received 192.5 μM of liposomes, what corresponds to a concentration of 7.7 mM PL/kg body weight (25 g × 40).

2.3. Fluorescence reflectance imaging

Organs (liver, kidneys, spleen, intestine, lung, heart, muscle, brain, and bone) of mice that were sacrificed 72 h after the injection of 80 nM/kg liposomes were scanned *ex vivo* (at 750 nm) for liposomal accumulation using a 2D Fluorescence Reflectance Imaging (FRI) (FMT2500 LX, PerkinElmer, Waltham, Massachusetts, USA). The total fluorescence of each organ was quantified in counts/energy (normalized to 100 mm^2/tissue).

2.4. Liver injury models

Liposomes and control solutions were injected intravenously at a volume of 100 μL. ConA-based hepatitis was induced after 40 h by injecting ConA (Sigmaaldrich, St. Louis, USA) at 15 mg/kg intravenously, and sacrificing mice eight hours later. Chronic liver injury was induced using repetitive intraperitoneal CCl_4 (Merck, Darmstadt, Germany) challenge twice weekly for six weeks [11]. Control animals received the same volume of vehicle (corn oil). Mice were sacrificed 48 h after the last injection of CCl_4.

2.5. Liver enzymes, histology, and immunohistochemistry

ALT was assessed at 37 °C in serum using the Modular Preanalytics System (Roche, Penzberg, Germany). Hematoxylin and Eosin (H&E) and Sirius Red stainings were done following established protocols. Sirius Red stained sections were analyzed by morphometrical assessment of the area fraction. Staining of CD45 and F4/80, and α smooth muscle actin (αSMA) was done according to optimized protocols [20].

2.6. Cell isolation, flow cytometry, and fluorescence microscopy

Blood was taken from the right ventricle. Red blood cell lysis was done using Pharm Lyse (BD, Franklin Lakes, USA) and was stopped using Hank's buffer salt solution (HBSS) supplemented with 5 μM ethylenediaminetetraacetic acid and 0.5% bovine serum albumin. Hepatic leukocytes were isolated from liver as described earlier [11]. Single cell suspensions were filtered using a 100 μM mesh, and stained for flow cytometry as described earlier in detail [11]. Additionally, count beads (calibrite beads, BD, Franklin Lakes, USA) were added to organ cell suspensions to determine cell numbers in different organs. Flow cytometric data are given as percentages of leukocytes or as absolute numbers calculated from organ weight or blood volume. To prepare sections for fluorescence microscopy, cryosections sizing 20 μM were prepared and analyzed using a Zeiss Axio Observer Z1 fluorescence microscope (Carl Zeiss, Oberkochen, Germany).

2.7. Cell viability and cell death assessment

Live-dead staining was done in 48 well plates according to the instructions of the manufacturer (Life Technologies, Carlsbad, CA, USA). To determine the mode of cell death, we used an Annexin V (conjugated with allophycocyanin) apoptosis detection kit (BD, Franklin Lakes, USA). Propidium iodide was used to stain necrotic cells in parallel (BD, Franklin Lakes, USA).

2.8. Gene expression analysis of liver tissue

Liver pieces were snap-frozen in liquid nitrogen, and RNA was purified using the peqGold kit (PEQLAB Biotechnologie GmbH, Erlangen, Germany). Complementary DNA was generated from RNA using the First Strand cDNA synthesis kit (Roche, Penzberg, Germany). Quantitative real-time polymerase chain reaction was done based on SYBR Green reagent (Roche, Penzberg, Germany). Reactions were done as triplicates, and β-actin was used to normalize gene expression. Primer sequences are available upon request.

2.9. Statistical analysis

Statistical analysis was done using GraphPad prism 5 using appropriate statistical tests, as indicated in the figure legends.

3. Results and discussion

3.1. Biodistribution of liposomes on an organ and cellular level

To study the biodistrubution of liposomes *in vivo*, we performed FRI *ex vivo* scans of bone, brain, muscle, heart, lung, intestine, spleen, kidney, and liver (Fig. 1(A)). Quantifications of fluorescence clearly revealed that the liver is the predominant organ for liposome uptake. The relatively high amount of nanocarriers in kidney may be partially explained by free dye occurring during liposome disintegration *in vivo* as the size of the liposomes (100 nm) exceeds the limit of renal clearance (Fig. 1(B)). Already twenty-four hours after intravenous injection in mice, fluorescently tagged liposomes predominantly accumulated in the liver, where they were widely distributed. In spleen, liposomes were mostly located in the white pulp (Fig. 1(C)). When we subjected cells from various tissues, including liver, spleen, blood, and bone marrow to flow cytometry, we found that liposomes mostly accumulated in the liver in a dose-dependent manner (Fig. 1(D)). On the contrary, the systemic distribution of liposomes was restricted to very high doses based on the mean fluorescence intensity (MFI) of the fluorescence signal (Fig. 1(E)).

To unravel the exact cellular distribution of the liposomes, we performed multiplex antibody co-stainings of selected organs, which allowed for a flow cytometry-based quantification of the internalization of the fluorescently labeled liposomes by distinct immune cell subpopulations. As anticipated from earlier studies [21], liposomes mostly accumulated in monocytes and

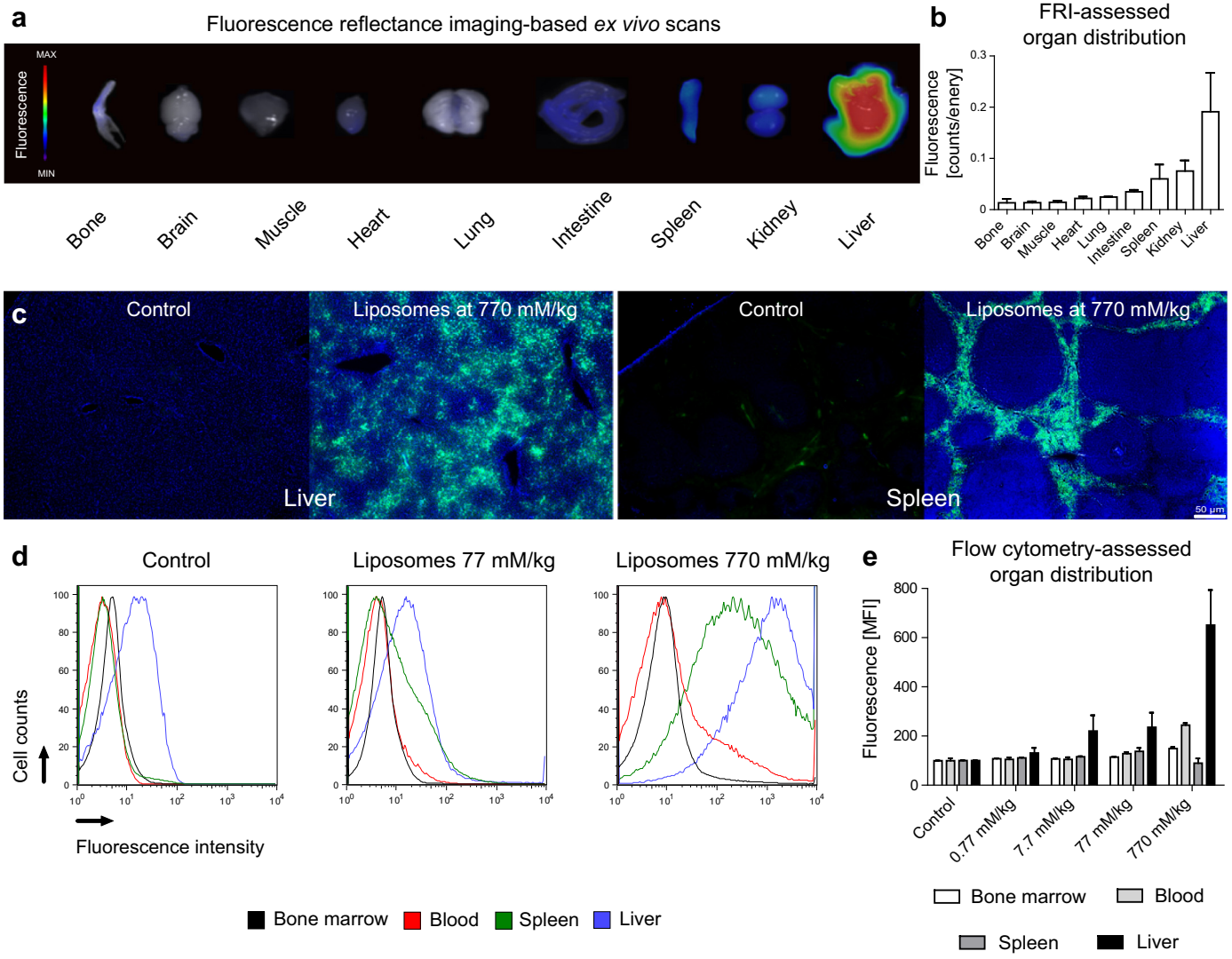

Fig. 1. Liposome distribution *in vivo*. Fluorescent liposomes (labeled with NBD-PE and Alexa Fluor 750) or vehicle control (0.9% sodium chloride) were injected intravenously into 8–12 weeks old C57BL/6 wild-type ($n = 5$ mice *per* condition). Organs were scanned *ex vivo* at 750 nm wavelength using Fluorescence Reflectance Imaging (FRI), representative images are shown for each organ 72 h after liposome injection (a), and a statistical summary of fluorescence intensity is given as counts *per* energy of $n = 3$ different experiments, normalized on 100 mm^2 (b). Cryosections of liver and spleen reveal liposomes (green) (c),which were further quantified using the shift in the mean fluorescence intensity (MFI) by flow cytometry from isolated cells of different organs (d,e). (For interpretation of the references to color in this figure legend, the reader is referred to the web version of this article.)

macrophages, which were stained using CD11b and F4/80 in various tissues. However, at higher doses, liposomes were also detected in T cells and, to a lesser extent, in B cells (Fig. 2(A)). Because hepatic macrophages are potential target cells for liver therapies, we further distinguished liposome accumulation in either infiltrating inflammatory macrophages (iMΦ) or resident liver macrophages (specifically Kupffer cells [KC]), based on flow cytometry (Fig. 1(B)). At high concentrations, surprisingly, the liposomes mostly accumulated in iMΦ, whereas at the highest concentrations, liposomes were found both in KC and iMΦ (Fig. 1(C)).

3.2. Immunosuppressive and immune-modulatory effects of Dex liposomes in healthy mice

While it is well-known that immunosuppressive nanoparticles can affect hepatic macrophages [22], no comprehensive analysis of the effects of systemically administered Dex-containing liposomes on other immune cells such as blood lymphocytes has been performed. Such effects are considered to be meaningful as earlier studies suggested inhibitory effects of Dex liposomes on lymphocyte functionality *in vitro* [23]. In fact, Dex liposomes evoked a significant depletion of both CD4 and $CD8^+$ T cells in blood (Fig. 3(A)), an effect which was much stronger (about one log rank) than depletion by free Dex. Circulating B cells were reduced by Dex liposomes as well (Fig. 3(B)). Monocytes in blood were also efficiently reduced, yet, to a lower extent overall (Fig. 3(C)), whereas neutrophil counts increased upon Dex liposome treatment (Fig. 3(D)). This mild neutrophilia might be explained by a low-level liver injury caused by encapsulated Dex, because we also detected mildly increased levels of the enzymes aspartate aminotransferase (AST) and alanine aminotransferase (ALT) in serum that reflect liver injury (Supplementary Fig. S1). These mild toxic effects with high dose Dex liposomes were similar to earlier findings obtained with high dosages of gold nanoparticles [11]. Notably, the endotoxin content of all liposome batches used in this study was below the detection limit of a *Limulus amebocyte* lysate (LAL assay), and therefore, effects of bacterial components which might activate immune cells were excluded.

Gene expression analyses from liver tissue by quantitative real-time PCR demonstrated that Dex liposomes significantly inhibited proinflammatory mediators such as interleukin 1β (IL1β) and IL6 that are mostly produced by macrophages, but also of interferon γ (IFNγ), which is synthesized by helper T cells (Supplementary Fig. S2(A)). Additionally, the T cell-derived IL4 and IL10 were also reduced by Dex liposomes (Supplementary Fig. S2(B)), underlining

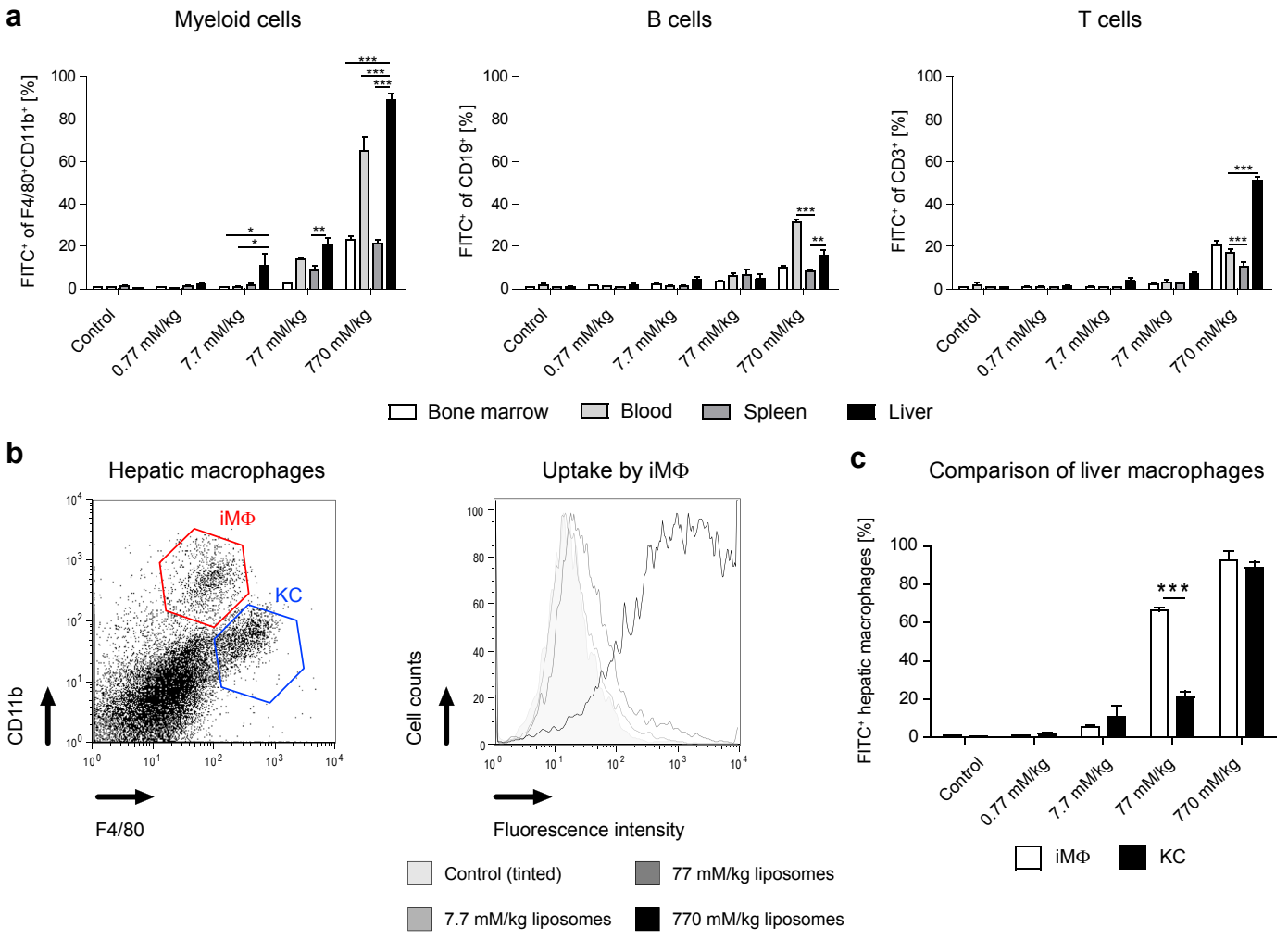

Fig. 2. Liposome distribution in immune cell populations *in vivo*. Fluorescent liposomes (labeled with NBD-PE) or vehicle control (0.9% sodium chloride) were injected intravenously into 8–12 weeks old C57BL/6 wild-type mice that were sacrificed after 24 h ($n = 5$ mice *per* condition). The cellular distribution of liposomes was determined by fluorescence signal and specific antibody co-staining using flow cytometry (a), flow cytometric analysis of hepatic macrophage subsets of liver (b), and localization in hepatic macrophage subsets (c). KC: Kupffer cells; iMΦ: inflammatory macrophages. Data represent mean ± SD; $^*P < 0.05$, $^{**}P < 0.01$, $^{***}P < 0.001$ (two-way ANOVA).

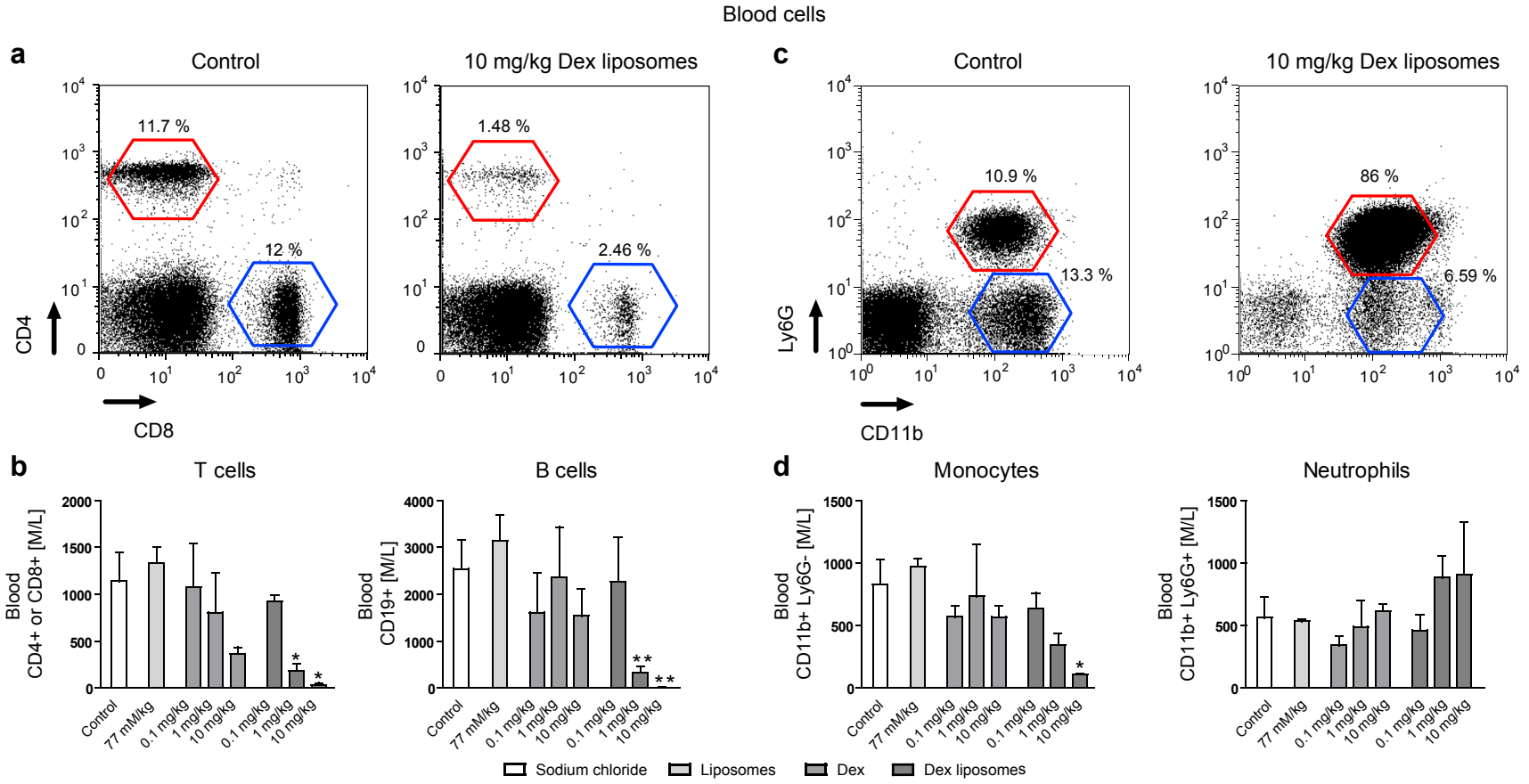

Fig. 3. Toxicity and blood immune cell alterations by dexamethasone-loaded liposomes *in vivo*. Empty liposomes, vehicle control (sodium chloride), free dexamethasone (Dex) or Dex liposomes were injected intravenously into 8-12 weeks old C57BL/6 wild-type mice 24 h before analysis ($n = 5$ mice *per* condition). Flow cytometric analysis of circulating T cells (representative plots, (a), and quantifications of T and B cell numbers (b). Analysis of blood monocytes and neutrophils using flow cytometry (representative plots, (c), and quantifications of both cell types (d). Data represent mean ± SD; $^{*}P < 0.05$, $^{**}P < 0.01$ (two-way ANOVA).

the broad spectrum of cytokine inhibition by glucocorticoids (GC) [24]. We further studied the immune cell subsets in spleen and observed similar immunosuppressive effects as in blood and liver, but to a lesser degree (Supplementary Fig. S3).

To study the effects of Dex and Dex liposomes on liver leukocytes, we performed immunohistochemical staining for the leukocyte marker CD45 on liver tissue. At the highest concentrations, Dex liposomes reduced the numbers of hepatic leukocytes (Fig. 4(A)), which was confirmed by flow cytometric determination (Fig. 4(B)). Upon flow cytometric phenotyping of leukocytes in the liver, T and B cells were found to be significantly reduced, whereas – as in blood – neutrophils were significantly increased at the highest dose of Dex liposomes (Fig. 4(B)). Staining of hepatic macrophages with the macrophage marker F4/80 revealed a reduction by Dex liposomes (Fig. 4(C)); this was almost exclusively related to reduced numbers of iMΦ but not of KC (Fig. 4(D), left). Similar to the monocyte depletion observed in blood, the iMΦ were significantly depleted by 10 mg/kg of free Dex, as well as by 1 and 10 mg/kg of Dex-containing liposomes (Dex-equivalent doses; Fig. 4(D)). In addition to their reduction in number, the iMΦ in the liver were also polarized towards the alternatively activated (anti-inflammatory) M2 subtype, as reflected by expression of the M2 markers CD124, CD206 and CD301 upon treatment with Dex liposomes (Fig. 4(E)).

3.3. Treatment of chronic liver injury and fibrosis using Dex liposomes

Due to the strong depletion of T and B cells and the efficient polarization of macrophages at 1 mg/kg of Dex liposomes, this dose of dexamethasone was used for subsequent experiments in mouse models of liver diseases. We first employed a model of chronic toxic liver injury by repetitive injections of CCl_4, which selectively kills hepatocytes and serves as a reliable model of liver fibrosis [25]. The CCl_4 injections were done twice weekly for six weeks, and Dex or Dex liposomes were administered starting from the third week of CCl_4 damage, to simulate therapeutic intervention in chronic liver injury. We found a significant reduction of liver damage in histology, reflected by reduced necrotic areas, in mice treated with Dex or Dex liposomes for 4 weeks (Fig. 5(A)), supported by reductions in the serum liver injury indicators AST and ALT (Fig. 5(B)).

Patients with chronic liver diseases are particularly hampered by progressive scarring of the liver as an aberrant wound healing reaction, termed liver fibrosis [26]. To assess the effects of the glucocorticoid-based drugs on progressive liver fibrogenesis, we performed immunohistochemical staining of αSMA, an indicator of hepatic stellate cell (HSC) activation (Fig. 6(A)), and of extracellular collagen fibers, the hallmark of fibrosis (Fig. 6(B)). Treatment with Dex and Dex-loaded liposomes significantly reduced HSC activation and collagen accumulation in chronic liver injury. Quantifications of Sirius Red staining indicated that Dex liposomes more efficiently reduced the collagen content in the liver compared to free Dex, while hepatic gene expression levels αSMA and collagen 1 (Col1A1) were similarly reduced in Dex and Dex liposome treated animals (Fig. 6(C)). According to the immunohistochemical staining of liver tissue for CD45, hepatic leukocytes were strongly reduced upon Dex and Dex liposome treatment during chronic liver injury (Fig. 6(D)). Surprisingly, T cells were the most affected cell type by flow cytometric analysis, while Kupffer cells even increased due to the treatment with Dex liposomes (Fig. 6(E)), coherent with earlier findings of a mild activation of human terminally differentiated macrophages after incubation with Dex liposomes [4]. The Dex liposomes led to a pronounced increase in the number of $CD301^+$ iMΦ (Fig. 6(F)), similar to the M2 polarizing effects observed in healthy mice (Fig. 4(E)). By mRNA expression analysis of whole liver tissue, IFNγ, which mainly originates from activated T cells, but not anti-inflammatory IL10, was found to be strongly reduced by the Dex-loaded liposomes (Fig. 6(G)), further supporting the role of T cells as cellular targets of Dex liposomes.

3.4. Dex liposome administration protects from immune-mediated hepatitis

As systemically administered corticosteroids are the first choice for the treatment of autoimmune hepatitis [27], we next evaluated the efficacy of Dex or Dex liposomes in an experimental model of acute liver injury based on Concanavalin A (ConA), which serves as a mouse model of immune-mediated hepatitis [28]. When mice were treated with Dex or Dex liposomes and subjected to ConA-mediated hepatitis 40 h later, Dex liposomes but not the free Dex almost completely abolished liver damage, with nearly normalization of liver histopathology and reduced necrotic areas (Fig. 7(A)), as well as significantly reduced serum liver enzymes (Fig. 7(B)). Extensive flow cytometric analyses of blood leukocytes again demonstrated that T cells were significantly reduced by the Dex liposomes, whereas neutrophils were increased (Fig. 7(C)). The leukocyte infiltration into the liver was similar for all treatment groups, as shown by CD45-based immunohistochemical staining (Fig. 8(A)). Importantly, T cells were identified as the only cell type that was significantly reduced upon Dex liposome treatment (Fig. 8(B)). In line, only the Dex-loaded liposomes evoked a marked reduction in various cytokines after ConA-induced hepatitis (Supplementary Fig. S4), corroborating the notion that liposomal Dex efficiently suppressed the immune activation underlying liver injury.

3.5. Dex liposomes induce cell death in T cells, but not in macrophages

Altogether, our experiments indicate that hepatic T cells rather than macrophages were the decisive cell type that was efficiently targeted by Dex liposomes in experimental liver injury models. The prominent depletion of T cell counts in blood and liver prompted us to address the sensitivity of T cells, in comparison to macrophages, to Dex and Dex-loaded liposomes. We therefore generated macrophages from bone marrow cells and isolated T cells from the spleens of untreated mice. Both cell types were then incubated with different concentrations of Dex and Dex-loaded liposomes (1 μg/mL, 10 μg/mL, and 100 μg/mL), which corresponded to the concentrations used *in vivo* (0.1 mg/kg, 1 mg/kg, and 10 mg/kg), according to calculations described earlier [11,19]. As expected, T cells were indeed much more sensitive to Dex-induced cell death, as indicated by specific live-dead cell staining (Fig. 9(A)). T cells were highly susceptible to cell death induction already at low concentrations of Dex liposomes (1 μg/mL, which corresponds to an *in vivo* dosage of 1 mg/kg), but only at higher concentrations of free Dex (Fig. 9(B)). In contrast, the cell viability of bone marrow-derived primary mouse macrophages was unaffected by both compounds (Fig. 9(B)). As the high numbers of iMΦ during chronic liver injury result from infiltrating monocytes of bone marrow origin [29], our *in vitro* experiments are in good agreement with the observation that the iMΦ compartment in the liver was not quantitatively reduced by the Dex liposome treatment in the CCl_4 and ConA model. On the contrary, the ConA hepatitis model is dependent on hepatic T cell activation and accumulation [30], thereby explaining the strong effects of Dex liposomes by depleting T cells on the liver injury phenotype of this model *in vivo*.

Upon binding to the cytosolic glucocorticoid receptor, glucocorticoids activate and suppress a large number of important inflammatory mediators via transcriptional mechanisms [31], but

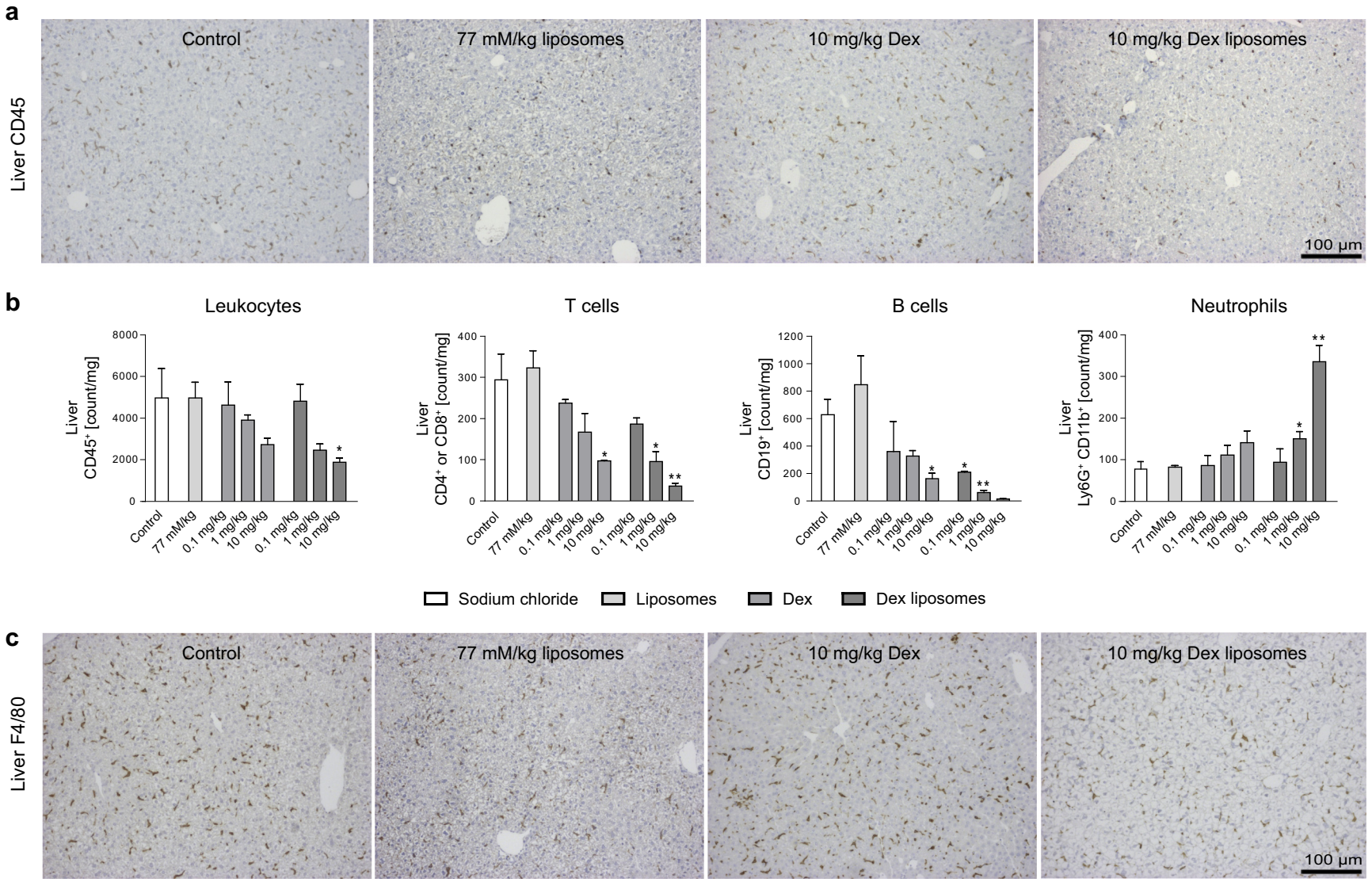

Fig. 4. Liver immune cell alterations by dexamethasone-loaded liposomes *in vivo*. Vehicle control (0.9% sodium chloride), liposomes (concentration given as mM/kg of liposome phospholipids), Dex, or Dex liposomes were injected intravenously into 8–12 weeks old C57BL/6 wild-type mice that were sacrificed after 24 h ($n = 5$ mice *per* condition).Hepatic immune cells were stained immunohistochemically using CD45 (leukocyte marker, in brown, (a), and immune cell subsets were quantified further using flow cytometry (b). Liver macrophages were stained using F4/80 (in brown, (c), and further analyzed using flow cytometry (d). Polarization of hepatic macrophages by Dex liposomes (e).Data represent mean ± SD; $^{*}P < 0.05$, $^{**}P < 0.01$, $^{***}P < 0.001$ (two-way ANOVA). (For interpretation of the references to color in this figure legend, the reader is referred to the web version of this article.)

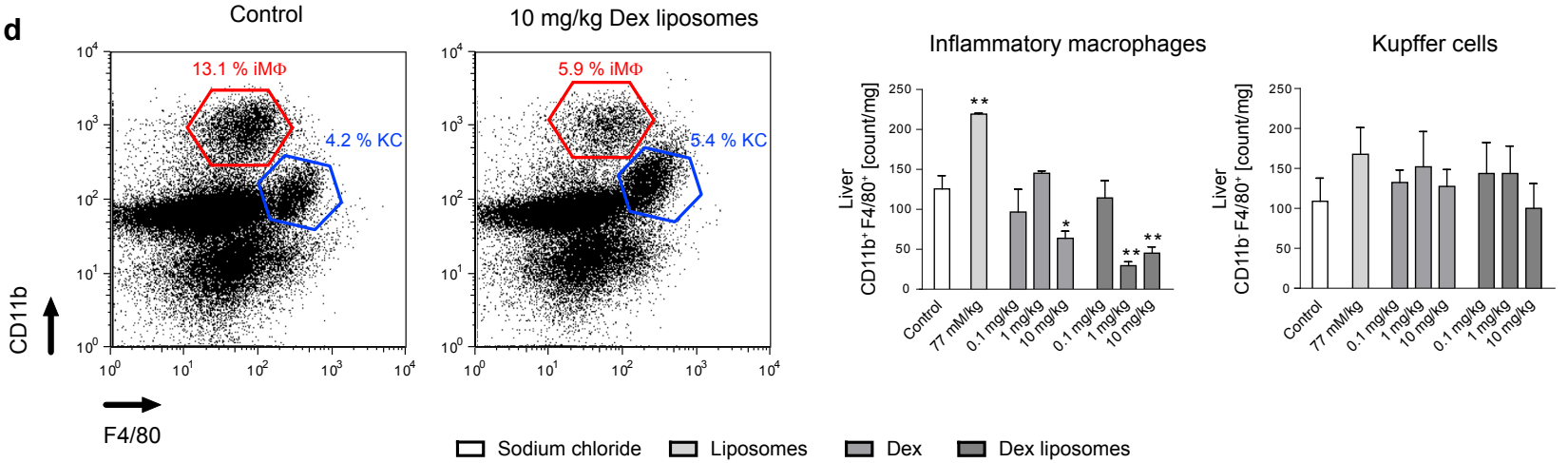

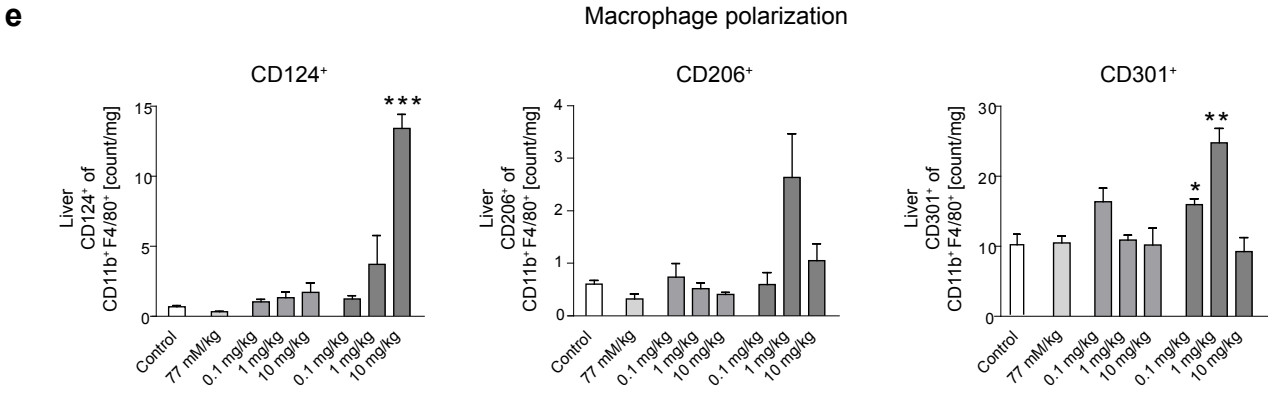

Fig. 4. (*continued*).

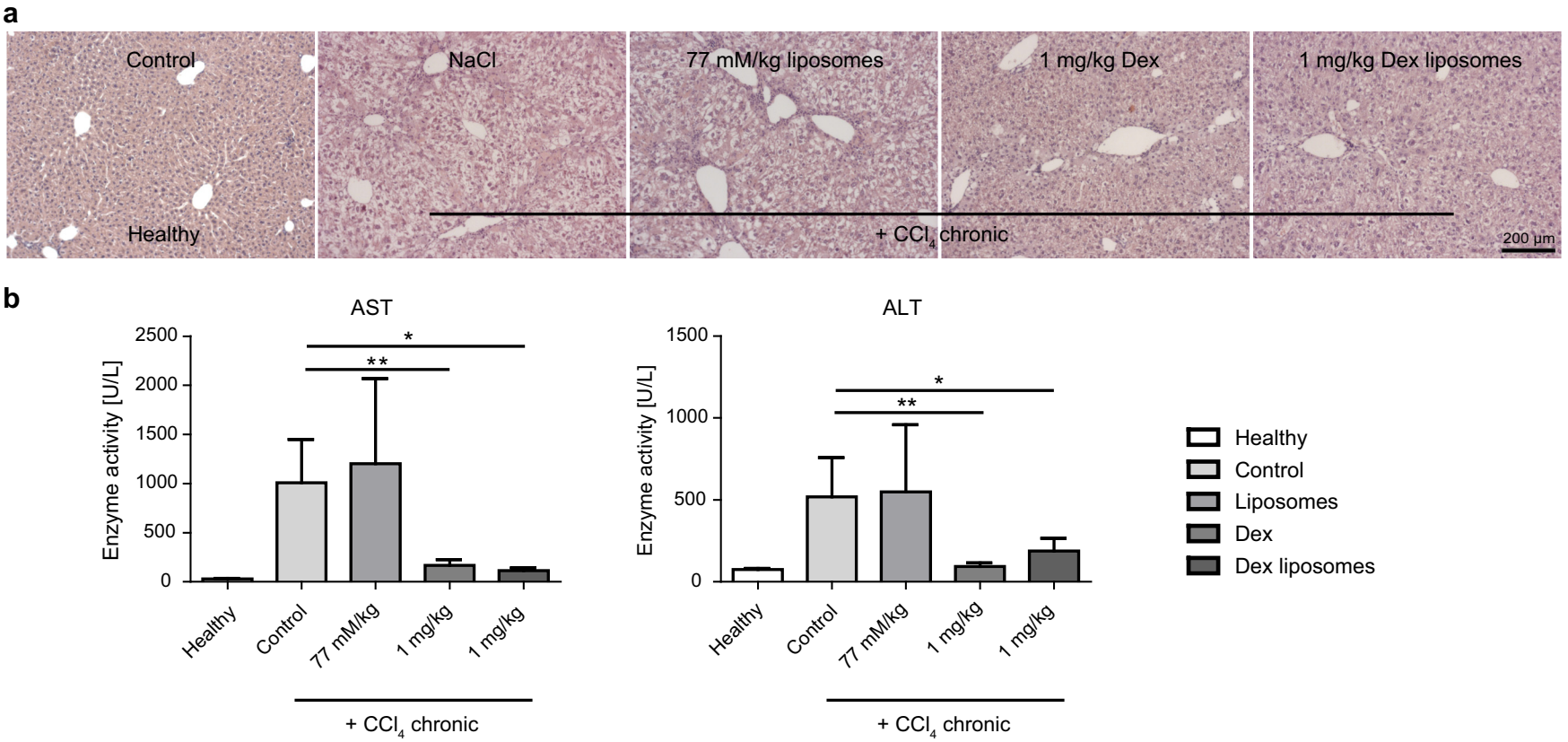

Fig. 5. Effects of dexamethasone-loaded liposomes on chronic liver injury *in vivo*. Chronic toxic liver injury was induced by six weeks of carbon tetrachloride (CCl_4) treatment of C57BL/6 mice ($n = 5$ mice *per* condition). Vehicle control (0.9% sodium chloride), liposomes (at a dose corresponding to 10 mg/kg Dex liposomes), free Dex, or Dex-loaded liposomes were administered intravenously weekly, starting from the third week after the induction of liver injury. Representative micrographs of hematoxylin and eosin staining of liver sections (a), and serum levels of aspartate (AST) and alanine (ALT) aminotransferase activity reflecting liver injury (b).Data represent mean ± SD; $^{*}P < 0.05$, $^{**}P < 0.01$, $^{***}P < 0.001$ (one-way ANOVA).

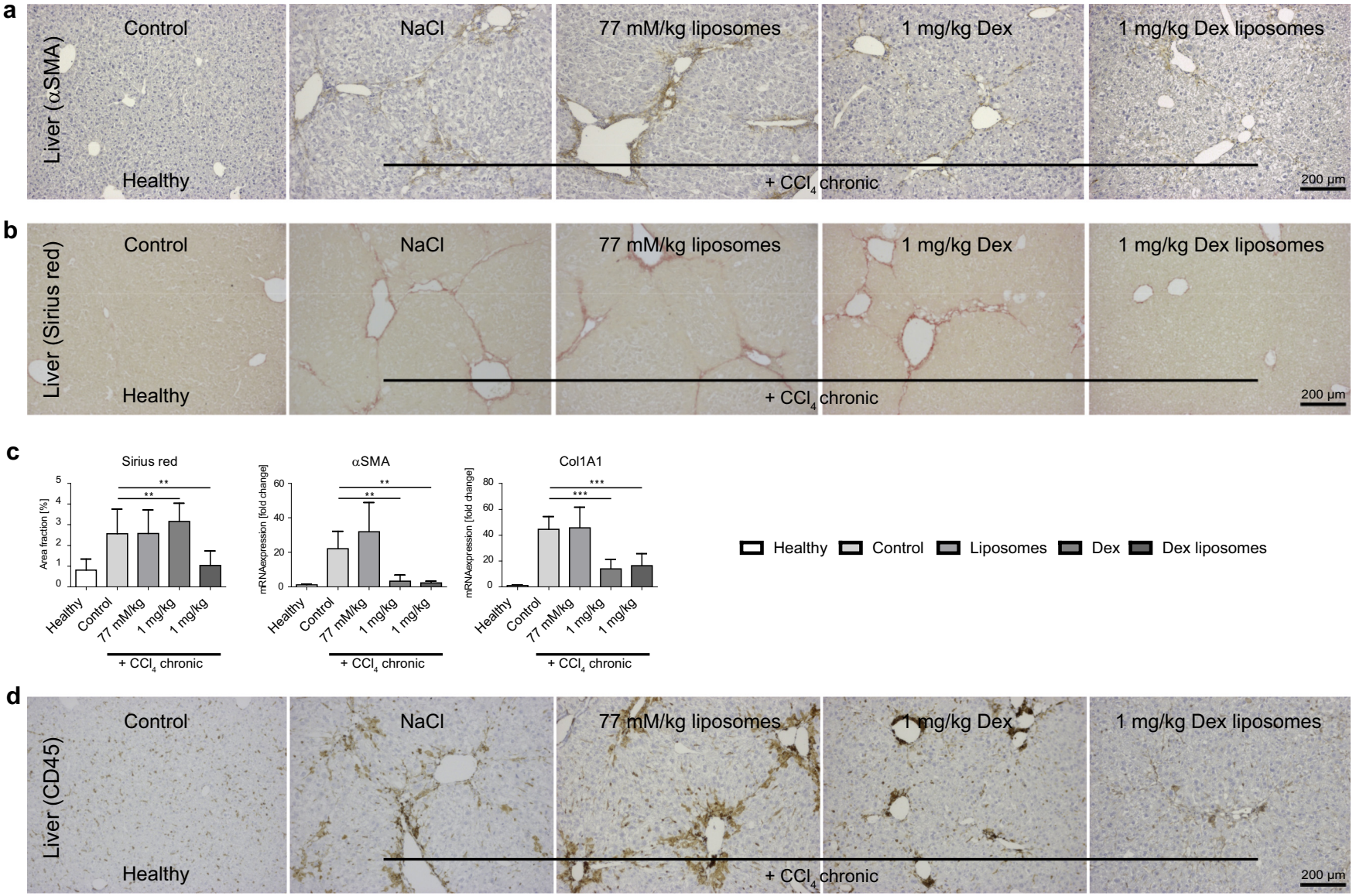

Fig. 6. Effects of dexamethasone-loaded liposomes on liver fibrosis *in vivo*. Chronic toxic liver injury was induced by six weeks of carbon tetrachloride (CCl_4) treatment of C57BL/6 mice ($n = 5$ mice *per* condition). Control treatment was done using the CCl_4 carrier (corn oil). PEGylated liposomes sizing 100 nm, Dex, or Dex liposomes were administered weekly starting from the third week of CCl_4 treatment. Hepatic stellate cell activation was studied by α smooth muscle actin (αSMA) staining (a). Sirius Red staining was performed, which reflects collagen deposition (b). Morphometric quantifications of Sirius Red staining, and quantifications of αSMA and Collagen 1A1 mRNA expression (c). Leukocyte infiltration was assessed by CD45 immunohistochemistry (d), alongside flow cytometric quantifications of liver immune cell subpopulations (e). Surface marker expression of hepatic inflammatory macrophages (f), and interferon γ (IFNγ) and interleukin 10 (IL10) mRNA expression from liver (g). Data represent mean ± SD; $^{*}P < 0.05$, $^{**}P < 0.01$, $^{***}P < 0.001$ (one-way ANOVA). (For interpretation of the references to color in this figure legend, the reader is referred to the web version of this article.)

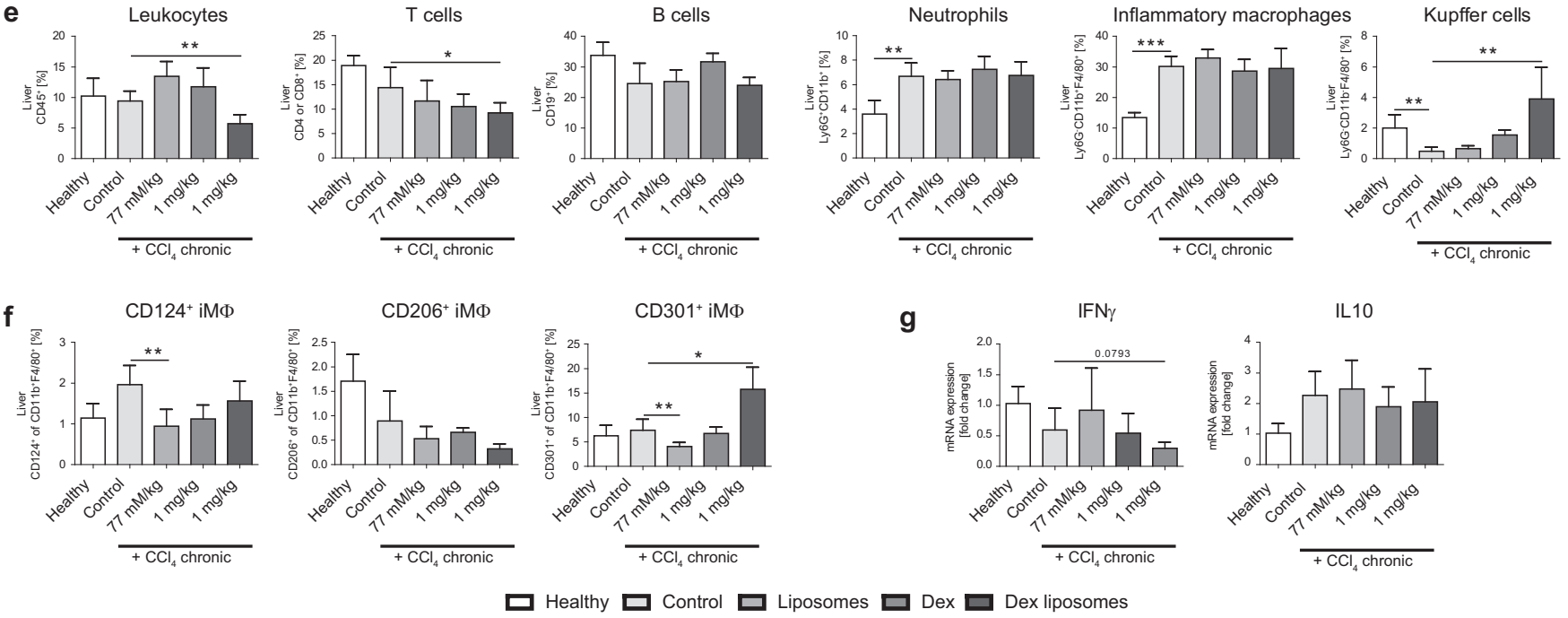

Fig. 6. (*continued*).

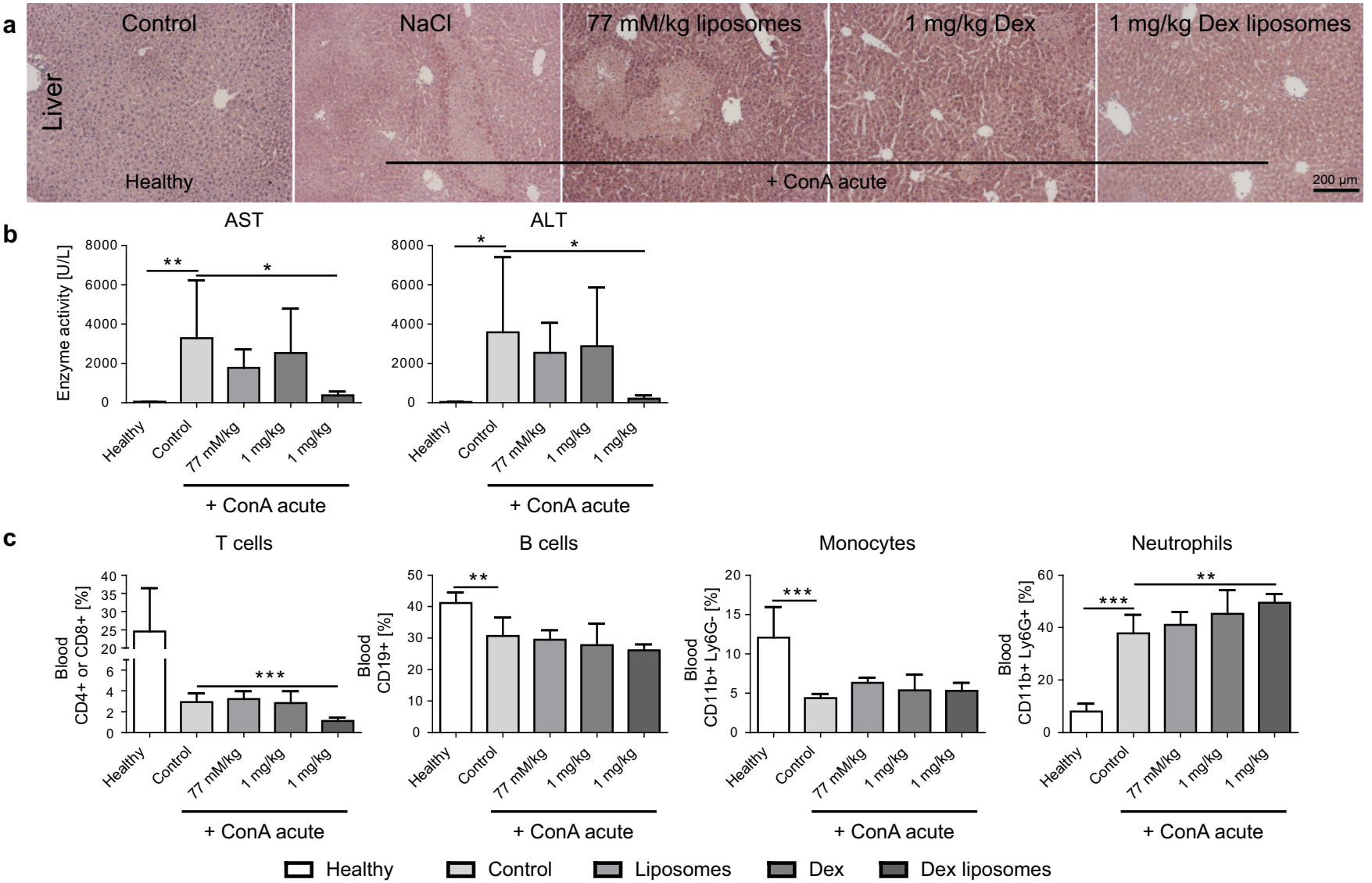

Fig. 7. Effects of dexamethasone-loaded liposomes on experimental immune-mediated hepatitis *in vivo*. Eight weeks old male C57BL/6 mice were treated with vehicle control (0.9% sodium chloride) 100 nm sizing liposomes, dexamethasone (Dex), or liposomal Dex intravenously, followed 40 h later of an intravenous injection of 15 mg/kg Concanavalin A (ConA). Mice ($n = 5$ *per* condition) were sacrificed eight hours after ConA injection. Hematoxilin and eosin staining of liver sections (please note that necrotic areas appear lighter) (a). Serum aspartate aminotransferase (AST) and alanine transaminase (ALT) activity reflect liver injury (b). Flow cytometric analysis of T cells, B cells, monocytes, and neutrophils in the blood (c). Data represent mean ± SD; $^{*}P < 0.05$, $^{**}P < 0.01$, $^{***}P < 0.001$ (one-way ANOVA).

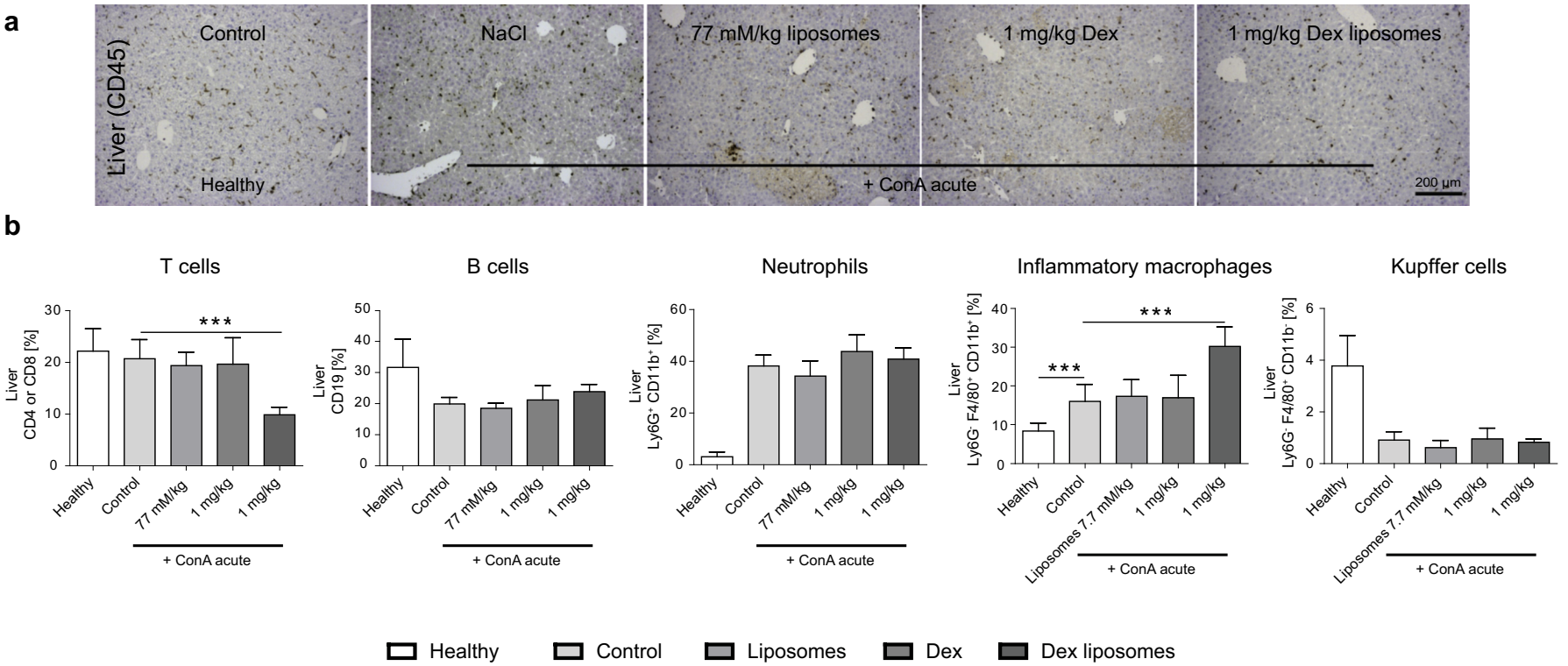

Fig. 8. Effects of dexamethasone-loaded liposomes on intrahepatic immune cell populations in experimental hepatitis *in vivo*. Eight weeks old C57BL/6 mice were treated with vehicle, control liposomes, dexamethasone (Dex), and liposomal Dex intravenously, followed 40 h later by intravenous injection of 15 mg/kg Concanavalin A (ConA). Mice ($n = 5$ *per* condition) were sacrificed eight hours after ConA injection. CD45 immunohistochemical staining (a). Flow cytometric analysis of hepatic immune cell populations (b). Data represent mean ± SD; $^{***}P < 0.001$ (one-way ANOVA).

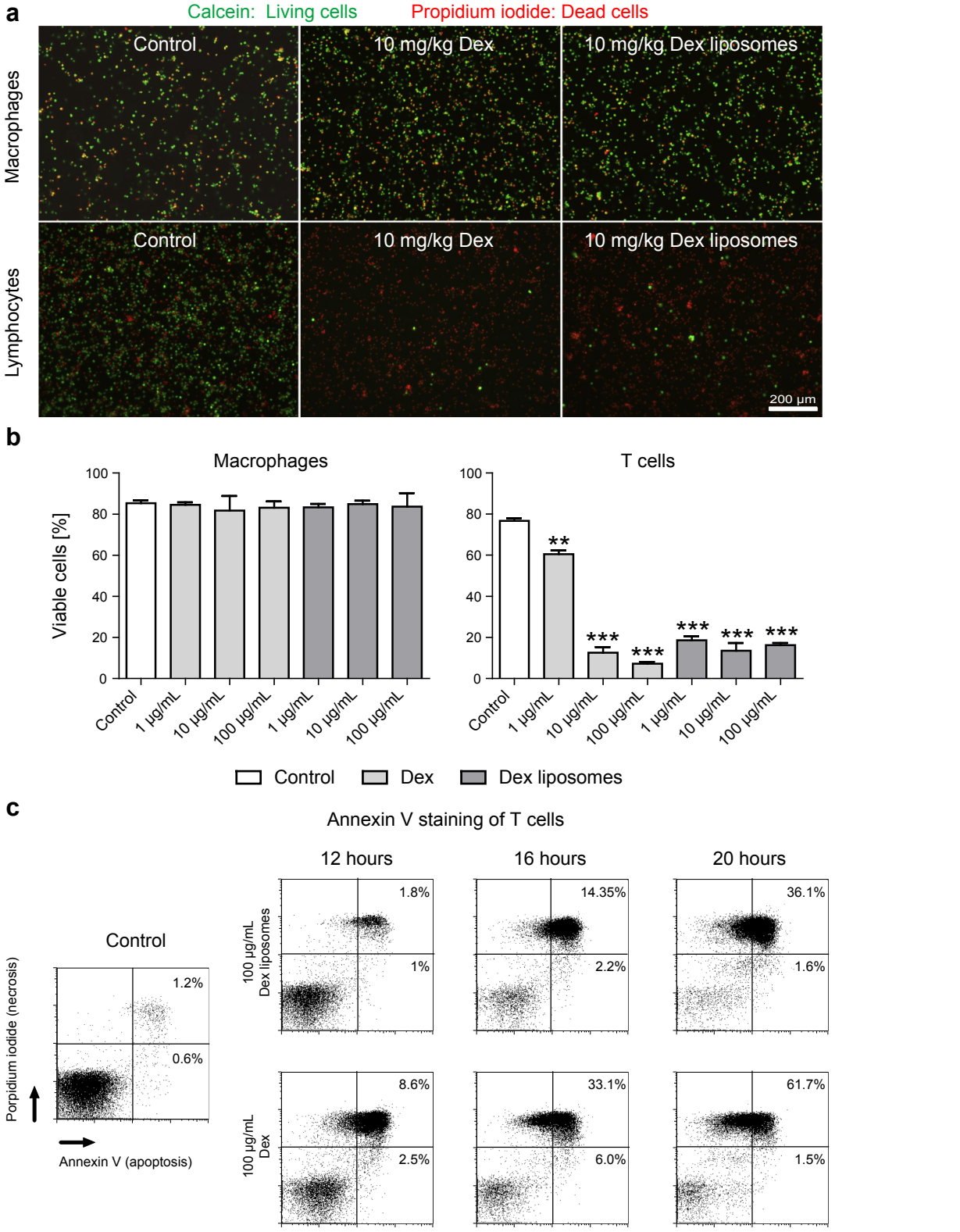

Fig. 9. Effects of dexamethasone-loaded liposomes on the viability of T cells and macrophages *in vitro*. Bone marrow-derived macrophages or splenicT cells were incubated for 24 h with either dexamethasone (Dex), or Dex liposomes and analyzed using live-dead staining (a). Statistical summary of live-dead staining of both cell types ($n = 5$ independent experiments) (b). Flow cytometric analysis of propidium iodide (necrotic cells) and Annexin V staining (apoptotic cells) of lymphocytes after incubation with Dex or Dex liposomes (representative plots, c).Data represent mean ± SD; $^{**}P < 0.01$, $^{***}P < 0.001$ (one-way ANOVA).

they are also known to trigger cell death pathways in leukocytes [32]. We therefore finally set out to explore the mechanism of dexamethasone-induced T cell depletion using propidium iodide (PI) and Annexin V staining. While PI staining identifies necrotic cells (as it penetrates the membrane of dead cells), Annexin V staining can be used to determine apoptosis based on surface phosphatidylserine expression [33]. Using the combination of Annexin V and PI, flow cytometry allows for distinguishing the type of cell death: viable cells stain negative for both Annexin V and PI, while cells which are in early apoptosis are Annexin^{+} and PI^{-}, whereas cells in late apoptosis or necrotic cells, on the other hand, are double positive. Interestingly, incubating T cells with Dex resulted in a short period of early apoptosis (bottom right quarter) with a rapid transition to late apoptosis and necrosis (top right and left quarters) (Fig. 9(C)). Similar to our earlier findings [4], liposomal encapsulation reduced the sensitivity of the T cells to Dex compared to free Dex, as indicated by an attenuated course of cell death (Supplementary Fig. S5) and a shift towards apoptotic in comparison to necrotic pathways especially at earlier time-points (Fig. 9(C)).

Our data corroborate the hypothesis that liposomal corticosteroids are highly suitable for treating inflammatory disorders [34], and expand this hypothesis to the treatment of acute and chronic inflammatory liver diseases. On the one hand, liposomes strongly accumulate in the liver, but they are not restricted to uptake by Kupffer cells [10,11,24], because liposomes target several immune cells including inflammatory macrophages and T lymphocytes. On the other hand, they not only endorse the anti-inflammatory differentiation of macrophages, generally referred to as M2 polarization, as anticipated from *in vitro* experiments [4], but they also promote the depletion of T cells. This latter mode of action might be of the utmost importance for the treatment of autoimmune hepatitis, as liposomal encapsulation could substantially reduce off-target effects compared with conventional corticosteroid treatment.

4. Conclusions

Virtually all nanomaterials strongly accumulate in the liver, which makes them interesting vehicles for treating liver diseases. Our study shows that liposomal dexamethasone may be suitable for targeting the liver as well as relevant intrahepatic immune cells. By depleting hepatic and systemic T cells, as well as by polarizing macrophages towards an anti-inflammatory phenotype, liposomal dexamethasone ameliorates acute and chronic experimental liver injury models. Thus, liposomal encapsulation enables an effective and selective delivery of dexamethasone to pathogenic immune cell populations in conditions of autoimmune mediated hepatitis.

Acknowledgments

This study was supported by a START grant from the RWTH Aachen (to M.B.), the German Research Foundation (DFG SFB/TRR 57, to F.T.), by the European Research Council (ERC Starting Grant 309495 — NeoNaNo; to T.L.), and by the Interdisciplinary Center for Clinical Research (IZKF) Aachen (to F.T.). The authors thank Mrs. Aline Roggenkamp, Carmen Tag, Sibille Sauer-Lehnen, and Louis van Bloois for excellent technical support.

Appendix A. Supplementary data

Supplementary data related to this article can be found at http://dx.doi.org/10.1016/j.biomaterials.2014.10.030.

References

[1] Goram AL, Richmond PL. Pegylated liposomal doxorubicin: tolerability and toxicity. Pharmacotherapy 2001;21:751–63.
[2] Crielaard BJ, Lammers T, Schiffelers RM, Storm G. Drug targeting systems for inflammatory disease: one for all, all for one. J Control Release 2012;161:225–34.
[3] Kawarabayashi N, Seki S, Hatsuse K, Kinoshita M, Takigawa T, Tsujimoto H, et al. Immunosuppression in the livers of mice with obstructive jaundice participates in their susceptibility to bacterial infection and tumor metastasis. Shock 2010;33:500–6.
[4] Bartneck M, Peters FM, Warzecha KT, Bienert M, van Bloois L, Trautwein C, et al. Liposomal encapsulation of dexamethasone modulates cytotoxicity, inflammatory cytokine response, and migratory properties of primary human macrophages. Nanomedicine 2014;10:1209–20.
[5] Karkhanis J, Verna EC, Chang MS, Stravitz RT, Schilsky M, Lee WM, et al. Steroid use in acute liver failure. Hepatology 2014;59:612–21.
[6] Nguyen-Khac E, Thevenot T, Piquet MA, Benferhat S, Goria O, Chatelain D, et al. Glucocorticoids plus N-acetylcysteine in severe alcoholic hepatitis. N Engl J Med 2011;365:1781–9.
[7] Longmire M, Choyke PL, Kobayashi H. Dendrimer-based contrast agents for molecular imaging. Curr Top Med Chem 2008;8:1180–6.
[8] Poelstra K, Prakash J, Beljaars L. Drug targeting to the diseased liver. J Control Release 2012;161:188–97.
[9] Tacke F, Zimmermann HW. Macrophage heterogeneity in liver injury and fibrosis. J Hepatol 2014;60:1090–6.
[10] Sadauskas E, Wallin H, Stoltenberg M, Vogel U, Doering P, Larsen A, et al. Kupffer cells are central in the removal of nanoparticles from the organism. Part Fibre Toxicol 2007;4:10.
[11] Bartneck M, Ritz T, Keul HA, Wambach M, Bornemann J, Gbureck U, et al. Peptide-functionalized gold nanorods increase liver injury in hepatitis. ACS Nano 2012;6:8767–77.
[12] Xue J, Schmidt SV, Sander J, Draffehn A, Krebs W, Quester I, et al. Transcriptome-based network analysis reveals a spectrum model of human macrophage activation. Immunity 2014;40:274–88.
[13] Raes G, Van den Bergh R, De Baetselier P, Ghassabeh GH, Scotton C, Locati M, et al. Arginase-1 and Ym1 are markers for murine, but not human, alternatively activated myeloid cells. J Immunol 2005;174:6561. author reply -2.
[14] Zimmermann HW, Tacke F. Modification of chemokine pathways and immune cell infiltration as a novel therapeutic approach in liver inflammation and fibrosis. Inflamm Allergy Drug Targets 2011;10:509–36.
[15] Herbert DR, Holscher C, Mohrs M, Arendse B, Schwegmann A, Radwanska M, et al. Alternative macrophage activation is essential for survival during schistosomiasis and downmodulates T helper 1 responses and immunopathology. Immunity 2004;20:623–35.
[16] Hope MJ, Bally MB, Webb G, Cullis PR. Production of large unilamellar vesicles by a rapid extrusion procedure: characterization of size distribution, trapped volume and ability to maintain a membrane potential. Biochim Biophys Acta 1985;812:55–65.
[17] Fiske CH, Subbarow Y. The colorimetric determination of phosphorus. J Biol Chem 1925;66:375–400.
[18] Rouser G, Fkeischer S, Yamamoto A. Two dimensional then layer chromatographic separation of polar lipids and determination of phospholipids by phosphorus analysis of spots. Lipids 1970;5:494–6.
[19] Bartneck M, Keul HA, Singh S, Czaja K, Bornemann J, Bockstaller M, et al. Rapid uptake of gold nanorods by primary human blood phagocytes and immunomodulatory effects of surface chemistry. ACS Nano 2010;4:3073–86.
[20] Baeck C, Wehr A, Karlmark KR, Heymann F, Vucur M, Gassler N, et al. Pharmacological inhibition of the chemokine CCL2 (MCP-1) diminishes liver macrophage infiltration and steatohepatitis in chronic hepatic injury. Gut 2012;61:416–26.
[21] Melgert BN, Olinga P, Van Der Laan JM, Weert B, Cho J, Schuppan D, et al. Targeting dexamethasone to Kupffer cells: effects on liver inflammation and fibrosis in rats. Hepatology 2001;34:719–28.
[22] Fichter M, Baier G, Dedters M, Pretsch L, Pietrzak-Nguyen A, Landfester K, et al. Nanocapsules generated out of a polymeric dexamethasone shell suppress the inflammatory response of liver macrophages. Nanomedicine 2013;9:1223–34.
[23] Benameur H, Latour N, Schandene L, Van Vooren JP, Flamion B, Legros FJ. Liposome-incorporated dexamethasone palmitate inhibits in-vitro lymphocyte response to mitogen. J Pharm Pharmacol 1995;47:812–7.
[24] Schweingruber N, Haine A, Tiede K, Karabinskaya A, van den Brandt J, Wust S, et al. Liposomal encapsulation of glucocorticoids alters their mode of action in the treatment of experimental autoimmune encephalomyelitis. J Immunol 2011;187:4310–8.
[25] Liedtke C, Luedde T, Sauerbruch T, Scholten D, Streetz K, Tacke F, et al. Experimental liver fibrosis research: update on animal models, legal issues and translational aspects. Fibrogenesis Tissue Repair 2013;6:19.
[26] Tacke F, Luedde T, Trautwein C. Inflammatory pathways in liver homeostasis and liver injury. Clin Rev Allergy Immunol 2009;36:4–12.
[27] Strassburg CP. Autoimmune hepatitis. Dig Dis 2013;31(1):155–63.
[28] Wang HX, Liu M, Weng SY, Li JJ, Xie C, He HL, et al. Immune mechanisms of concanavalin A model of autoimmune hepatitis. World J Gastroenterol WJG 2012;18:119–25.

[29] Karlmark KR, Weiskirchen R, Zimmermann HW, Gassler N, Ginhoux F, Weber C, et al. Hepatic recruitment of the inflammatory Gr1+ monocyte subset upon liver injury promotes hepatic fibrosis. Hepatology 2009;50:261–74.
[30] Tiegs G. Cellular and cytokine-mediated mechanisms of inflammation and its modulation in immune-mediated liver injury. Z fur Gastroenterol 2007;45:63–70.
[31] Stahn C, Buttgereit F. Genomic and nongenomic effects of glucocorticoids. Nat Clin Pract Rheumatol 2008;4:525–33.
[32] Herold MJ, Reichardt HM. Glucocorticoid-induced apoptosis in animal models of multiple sclerosis. Crit Rev Immunol 2013;33:183–202.
[33] Vermes I, Haanen C, Steffens-Nakken H, Reutelingsperger C. A novel assay for apoptosis. Flow cytometric detection of phosphatidylserine expression on early apoptotic cells using fluorescein labelled annexin V. J Immunol Methods 1995;184:39–51.
[34] Ozbakir B, Crielaard BJ, Metselaar JM, Storm G, Lammers T. Liposomal corticosteroids for the treatment of inflammatory disorders and cancer. J Control Release 2014;190:624–36.